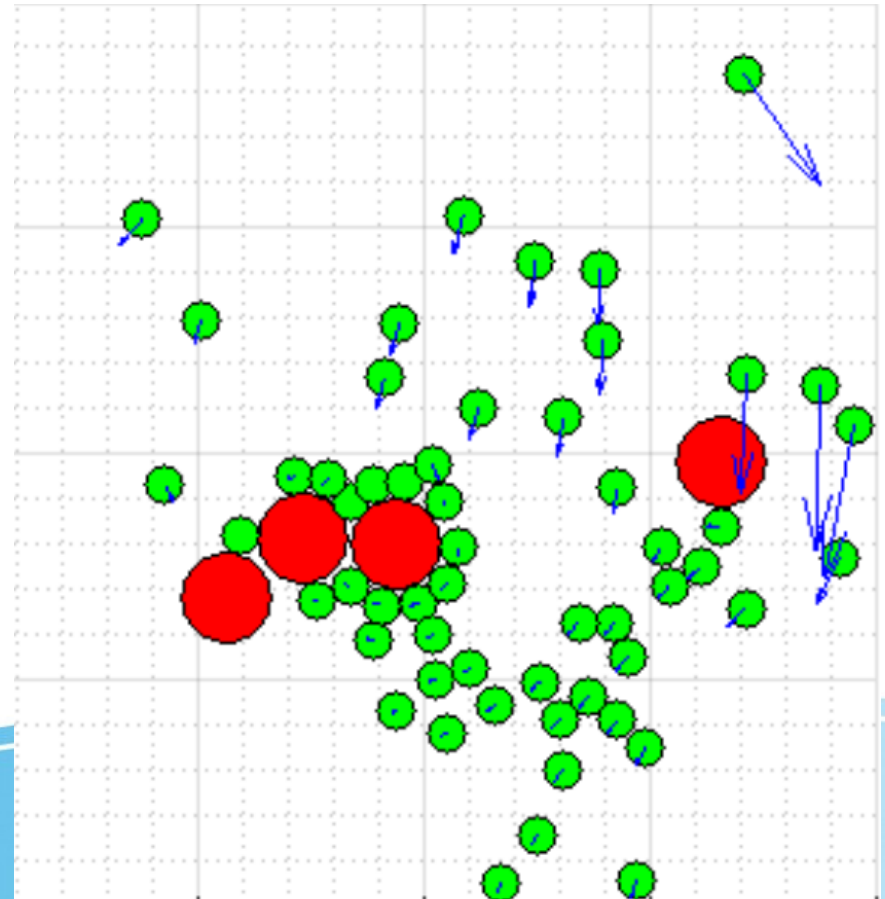


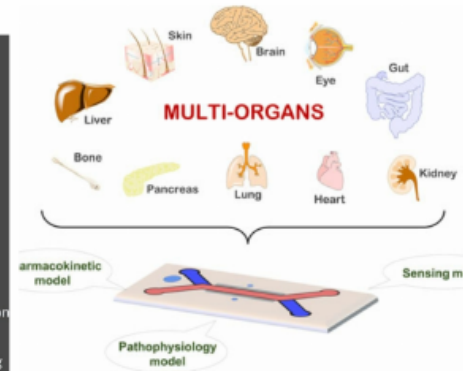
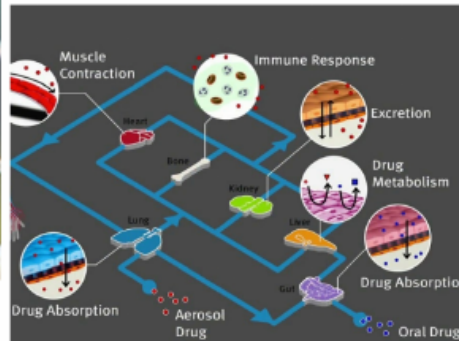
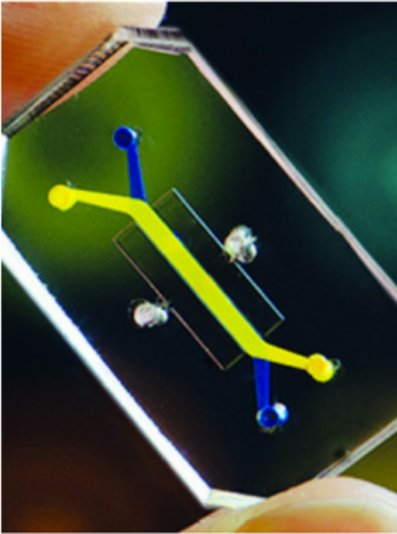
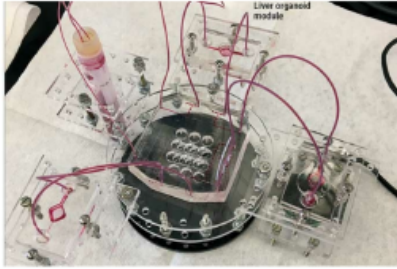
# Multiscale models of cell movements and their numerical approximation

Roberto Natalini  
Istituto per le Applicazioni del Calcolo  
Consiglio Nazionale delle Ricerche

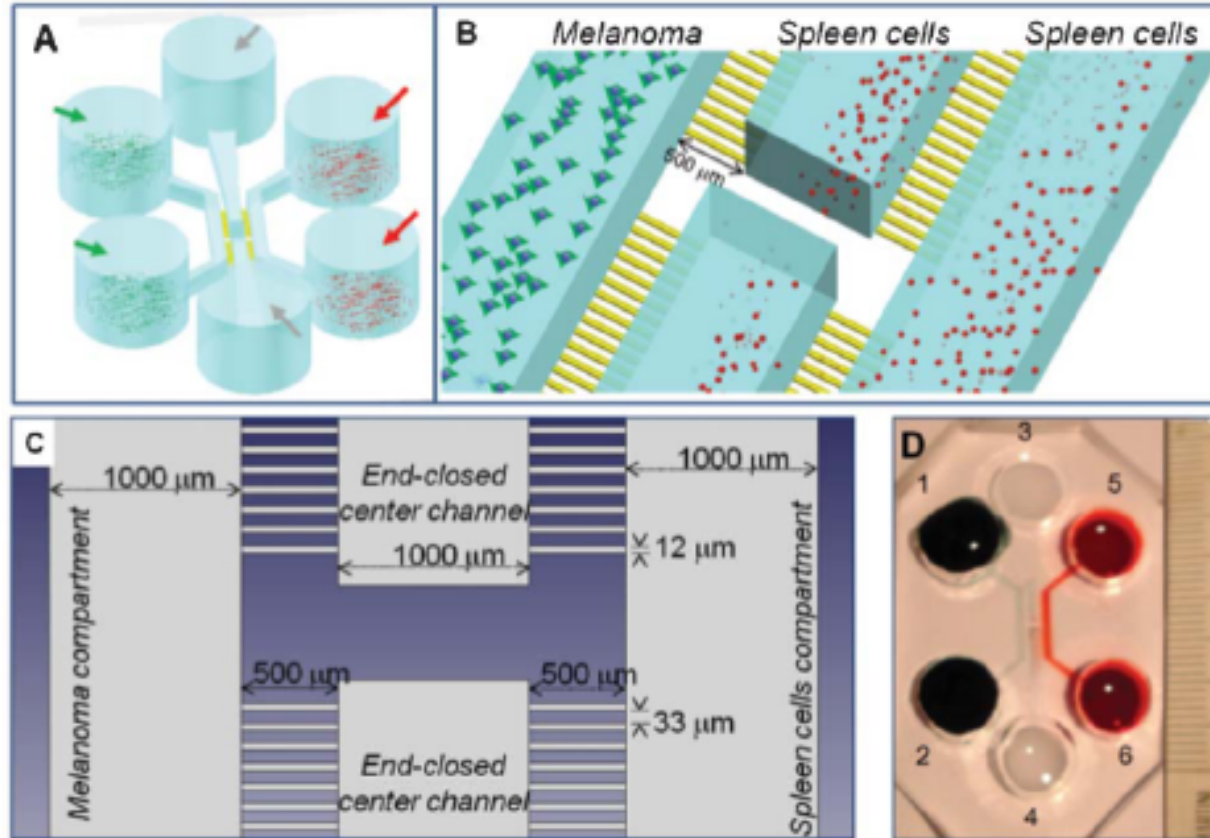
In collaboration with  
Gabriella Bretti (IAC-Cnr)  
Thierry Paul (Cnrs, Paris Sorbonne)  
Marta Menci (Uni. Campus-Biomedico)



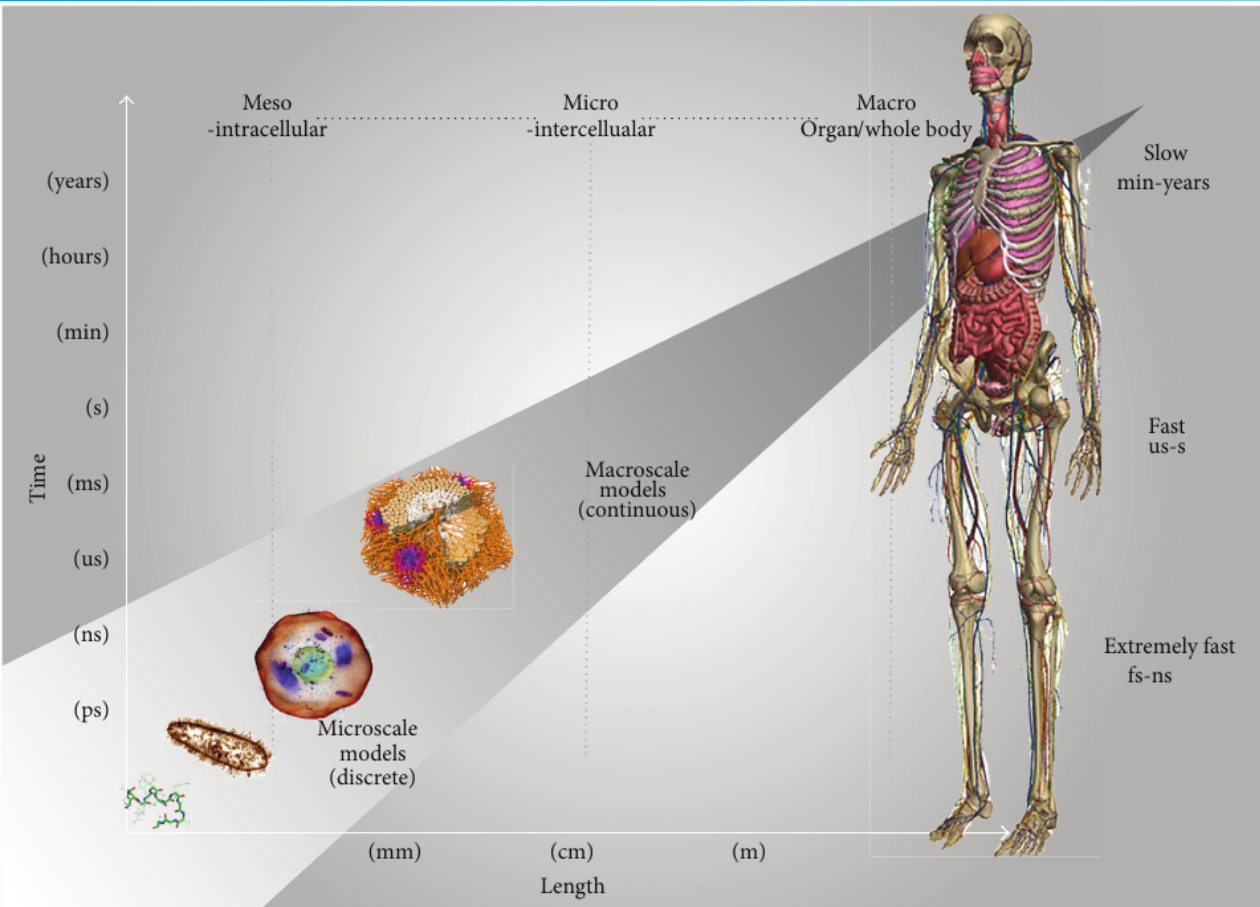
# Organs-on-chip and the new medicine



# Organs-on-chip and the new medicine



# The multiscale approach



- The real goal of these models is to use Organs-on-chip to predict the behaviour of real organs, so on the scale of billions of cells, using the data from the experiments at the microscale
- Create more realistic digital twins of our body
- It is crucial to keep the micro information in the memory of the macro models



# A crop of the full chip

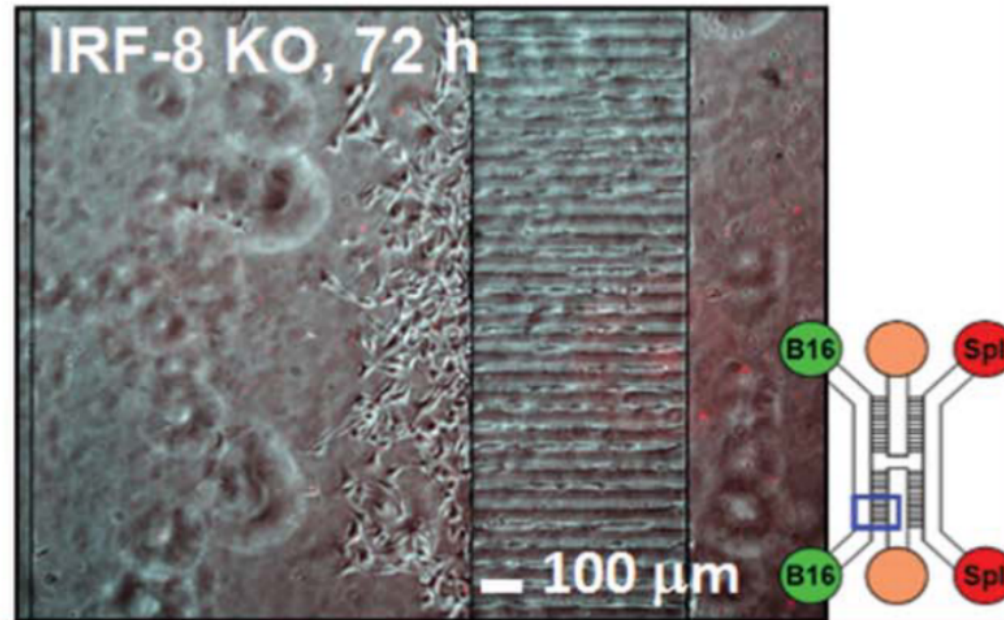
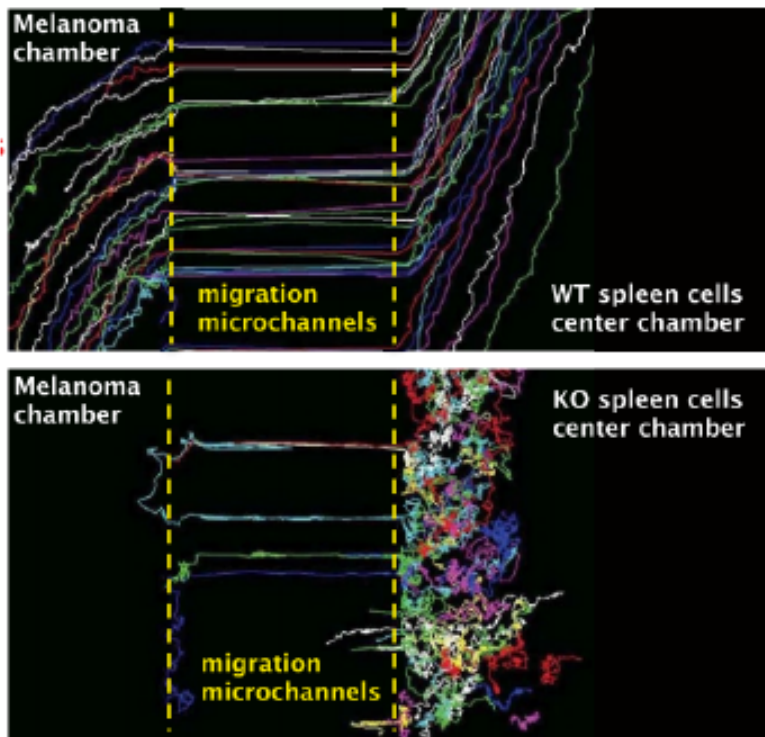


Figure: Crop of the microfluid chip after 72 hours

De Ninno A., Bertani F.R., Gerardino A., Schiavoni G., Musella M., Galassi C., Mattei F., Sistigu A., Businaro L. Microfluidic Co-Culture Models for Dissecting the Immune Response in in vitro Tumor Microenvironments. *J. Vis. Exp.* 170, e61895, doi:10.3791/61895, 2021



# Cell trajectories



Experiments (see Vacchelli et al: Science. (2015), Businaro et al: Lab on Chip rep.(2014))

- Tumour and KT/WT-type immune cells
- KO-type: uncorrelated random walk
- WT-type: strongly directed movement  $\Rightarrow$  Chemotaxis
- Tumour cells local sources of chemoattractant
- WT-type: Generation of tumour killing agent
- cytokine
- Chemical diffusion

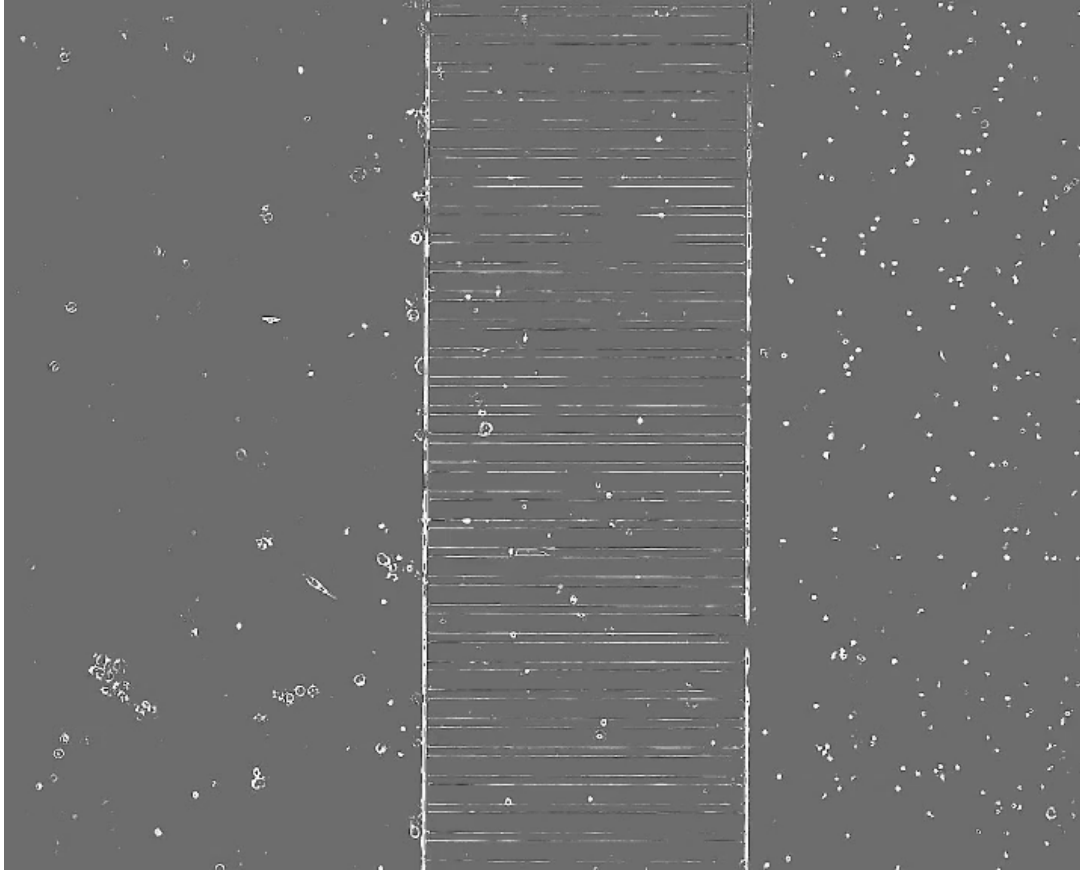
Available Data:

- Tumour and immune cell trajectories
- No information about chemical distribution

Cell trajectories performed by WT-cells and KO-type cells



# The time-lapse of the experiment



- $1702\mu\text{m} \times 1361\mu\text{m}$
- Duration: 48h-72h
- Cell movement: Diffusion and Chemotaxis
- Micro-channels allow only one cell to move through each.



# A first macroscopic model

Model(2D chamber) modified Keller-Segel model

$$\frac{\partial}{\partial t} T = D_T \Delta T - \lambda_T(\omega) T - k_T(t) T,$$

$$\frac{\partial}{\partial t} M = D_M \Delta M - \operatorname{div}(M \cdot \chi \nabla) - k_M(t) M,$$

$$\frac{\partial}{\partial t} \varphi = D_\varphi \Delta \varphi + \alpha_\varphi T - \beta_\varphi \varphi,$$

$$\frac{\partial}{\partial t} \omega = D_\omega \Delta \omega + \alpha_\omega M - \beta_\omega \omega,$$

Braun E.C., Bretti G., Natalini R. Mass-Preserving Approximation of a Chemotaxis Multi-Domain Transmission Model for Microfluidic Chips. *Mathematics*, 9(6)688, 1–34, 2021

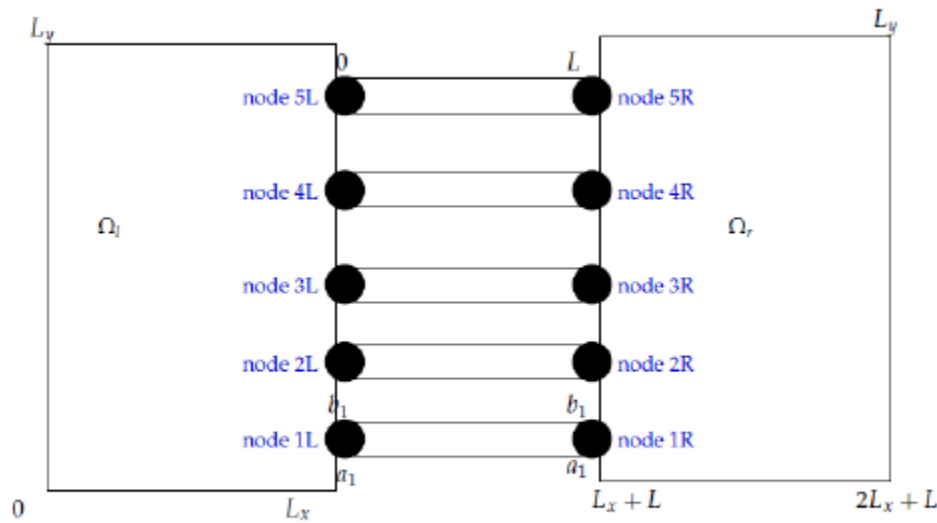


Figure: Numerical domain





# A first macroscopic model

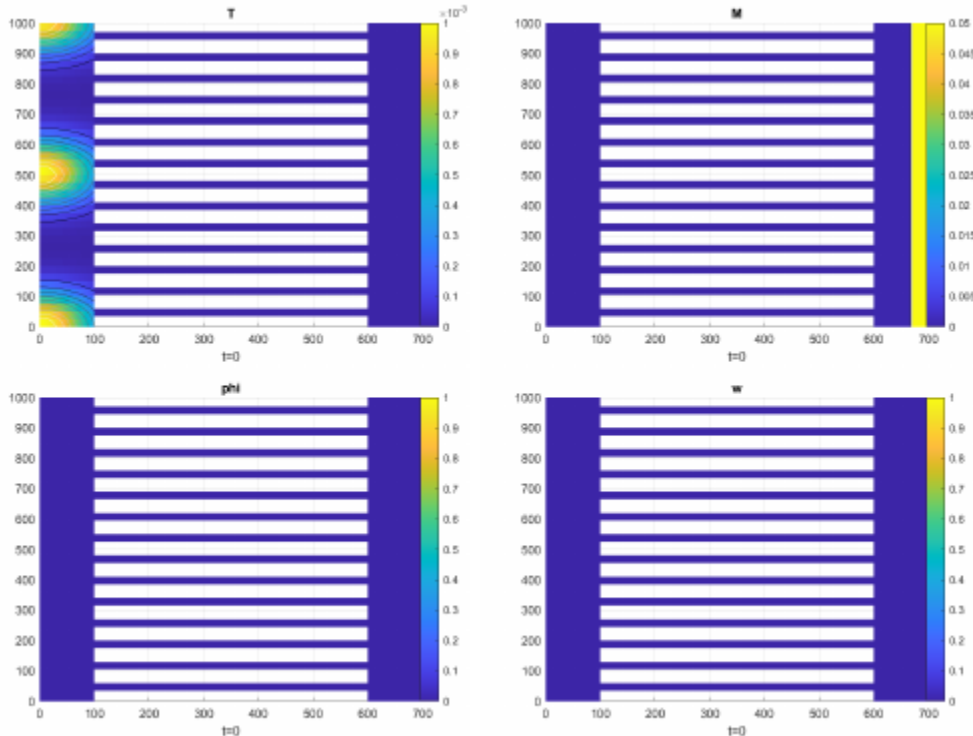


Figure: Initial distribution of  $T_0$ ,  $M_0$ ,  $\varphi_0$  and  $\omega_0$

- Implicit Crank-Nicolson method for diffusion term and source term
- Explicit central discretization for chemotactical convection term
- Artificial viscosity for improved stability in presence of high Péclet numbers
- Asymptotic Higher Order schemes(AHO) for the hyperbolic partial differential equation.
- Numerical boundary conditions that preserve the mass (for no-ux BC).
- Transmission condition of Kedem-Katchalski type (jump for density at interface)



# A first macroscopic model

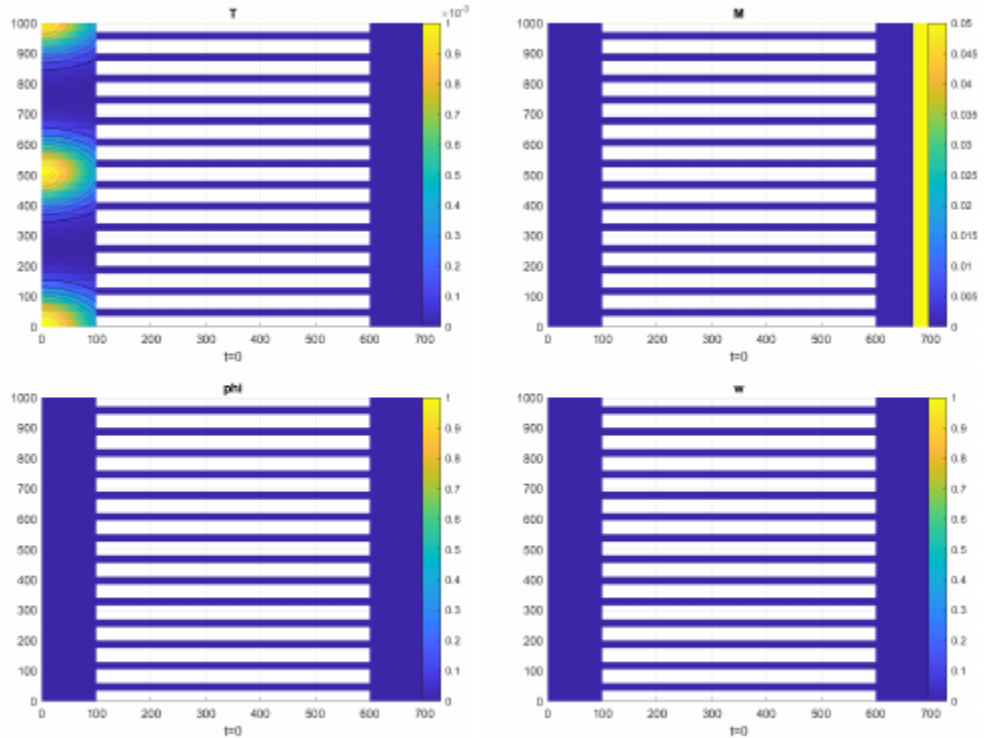
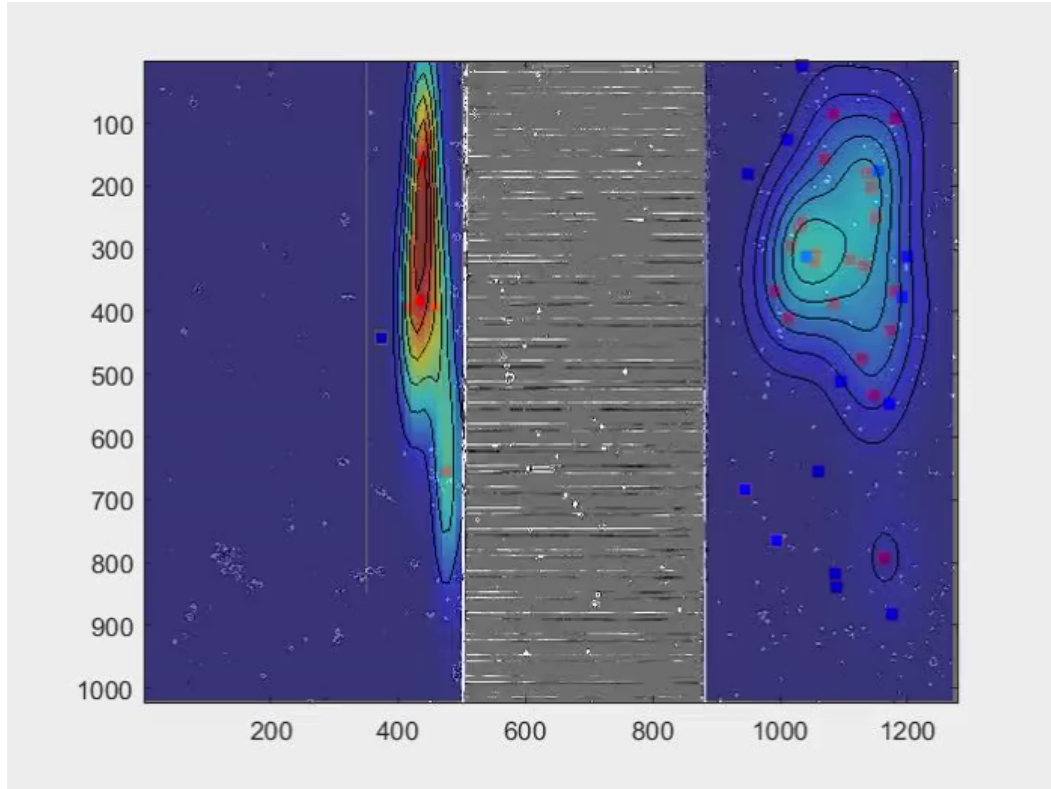
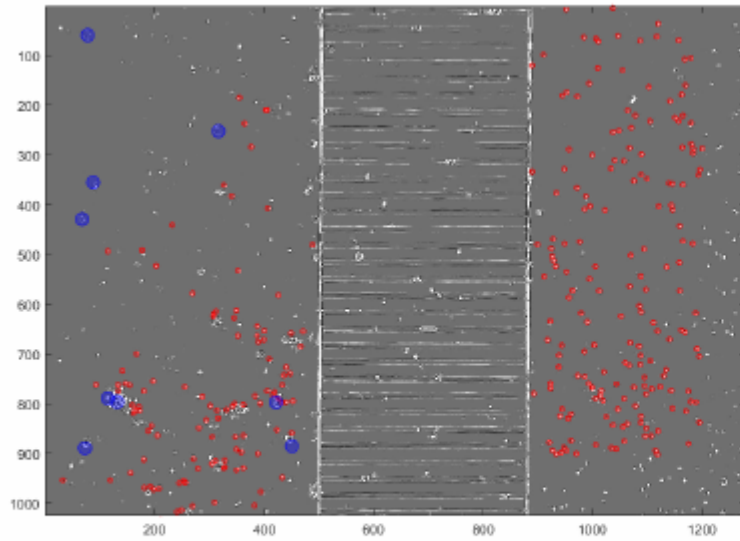


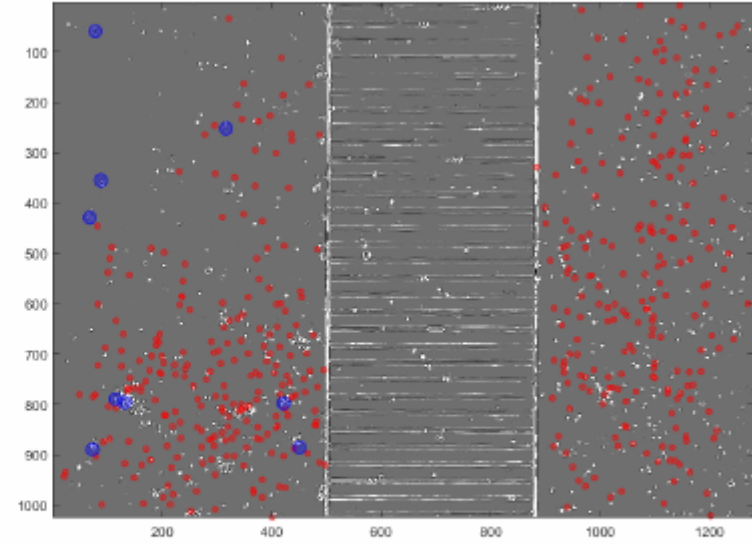
Figure: Initial distribution of  $T_0$ ,  $M_0$ ,  $\phi_0$  and  $w_0$



# Back to the experimental data



(a)

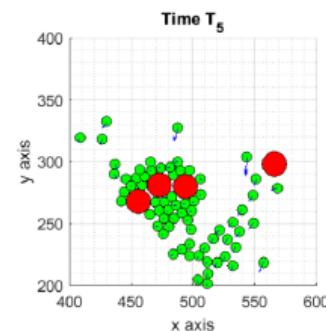
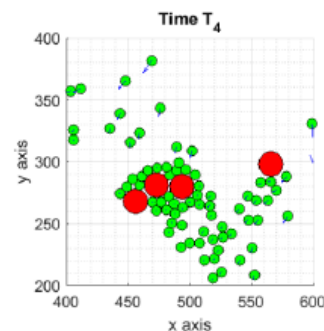
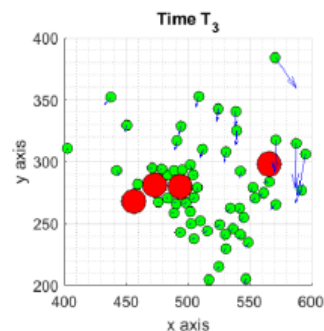
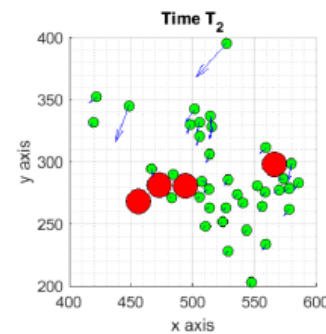
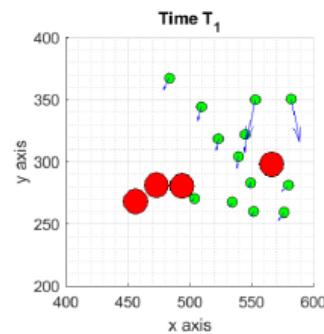
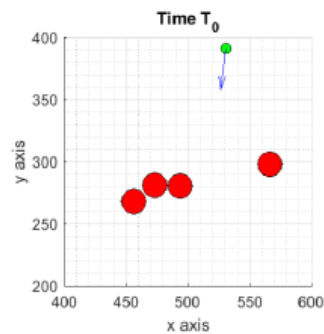
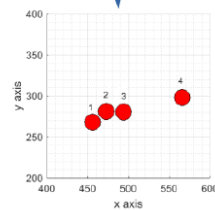
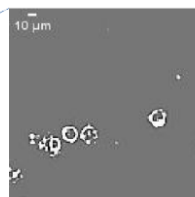
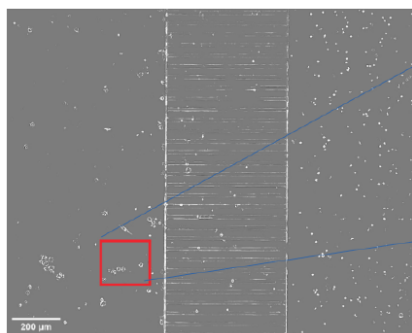


(b)

Figure: left: Tracked cell . Right: Artificially created cells.



# Beyond Keller-Segel: a micro-hybrid model



Gabriella Bretti, Adele De Ninno, Roberto Natalini, Daniele Peri and Nicole Roselli, Estimation Algorithm for a Hybrid PDE–ODE Model Inspired by Immunocompetent Cancer-on-Chip Experiment, *Axioms* 2021, 10(4), 243



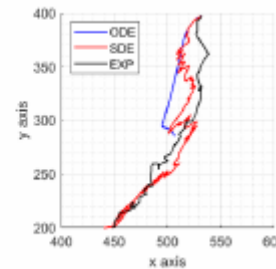
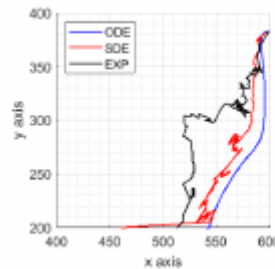
# A hybrid model

$X_i(t)$  : position of the  $i$ -th cell

$\phi(x, t)$  : concentration of the chemoattractant

$$\left\{ \begin{array}{l}
 \text{acceleration } i\text{-th cell} \\
 \ddot{X}_i \\
 \\
 \text{chemo rate in time} \\
 \partial_t \phi
 \end{array} \right. = \underbrace{\gamma F_1(\chi(\phi) \nabla \phi)}_{\text{chemotaxis}} + \underbrace{F_2(X, Y)}_{\text{immune/cancer}} + \underbrace{F_3(X)}_{\text{attraction/repulsion}} - \underbrace{\mu(\dot{X}_i - \sigma \psi)}_{\text{damping with noise}}$$

$$= \underbrace{D \Delta \phi}_{\text{diffusion}} + \underbrace{\xi F_4(Y)}_{\text{production cancer}} - \underbrace{\eta \phi}_{\text{molecular degradation}}$$



# A basic discrete model with chemotaxis

$$(1) \begin{cases} \dot{x}_i = v_i, \\ \dot{v}_i = \frac{1}{N} \sum_{j=1}^N \gamma(v_i - v_j, x_i - x_j) + \eta \nabla_x \varphi^t(x_i) \\ \partial_t \varphi = D \Delta \varphi - \kappa \varphi + f(x, X(t)) \end{cases}$$

- $x_i$  Position at time  $t$  of the  $i$ -th cell
- $v_i$  Velocity at time  $t$  of the  $i$ -th cell
- $\varphi$  Concentration of a chemoattractant produced by the cells
- $\gamma(v, x)$  Interaction function among the cells
- $f(x, X)$  Production of chemoattractant



# Main goals

- Study of the macroscopic behavior of the dynamical system
- Kinetic approach (Vlasov-type model): density of particles
- Hydrodynamic limit (Euler-type model): density of cells + velocity field:  
a numerical study

- without chemotaxis
- with chemotaxis



# The Cucker-Smale model (no chemistry)

$$(2) \begin{cases} \dot{x}_i = v_i, \\ \dot{v}_i = \frac{1}{N} \sum_{j=1}^N \psi(x_i - x_j)(v_j - v_i) \end{cases}$$

\* F. Cucker & S. Smale, IEEE T. Automat. Contr (2007)

\* S.Y. Ha & J.G. Liu, Commun Math Sci (2009)

time-asymptotic flocking

$$\lim_{t \rightarrow +\infty} \sum_{i=1}^N \|v_i(t) - v_{\text{CM}}(t)\|^2 = 0;$$

$$\psi(\xi) = \left( 1 + \frac{\|\xi\|^2}{R^2} \right)^{-\sigma}$$

$$\sup_{0 \leq t \leq +\infty} \sum_{i=1}^N \|x_i(t) - x_{\text{CM}}(t)\|^2 < +\infty$$





# The flow

The system (2) 
$$\begin{cases} \dot{x}_i = v_i, \\ \dot{v}_i = \frac{1}{N} \sum_{j=1}^N \psi(x_i - x_j)(v_j - v_i) \end{cases}$$

Generates a flow  $\Phi^t$  which is, given the initial data  $(x^{in}, v^{in}) = (x_1^{in}, \dots, x_N^{in}, v_1^{in}, \dots, v_N^{in})$

$$\Phi^t(x^{in}, v^{in}) = (x(t), v(t))$$



# A first mean field approach: the empirical measures

Given a solution  $(x(t), v(t))$  to system (2). The so-called empirical measure

$$\Pi_N^t(x, v) := \frac{1}{N} \sum_{i=1}^N \delta(x - x_i(t)) \delta(v - v_i(t))$$

is a special solution to the Vlasov equation:

$$(3) \partial_t \rho^t(x, v) + v \cdot \nabla_x \rho^t(x, v) + \nabla_v \cdot \left( \rho^t(x, v) \int_{2d} \psi(x - y)(v - w) \rho^t(y, w) dy dw \right) = 0$$

\* S.-Y. Ha, E. Tadmor, From particle to kinetic and hydrodynamic descriptions of flocking, *Kinet. Relat. Models* 1 (2008) 415-435

\* Carrillo, José A.; Choi, Young-Pil Mean-field limits: from particle descriptions to macroscopic equations. *Arch. Ration. Mech. Anal.* 24 (3) (2021) 1529-1573.



# The mean field limit: the empirical measures approach

**Theorem:** given an initial measure  $\rho^{in}$  such that  $\lim_{N \rightarrow \infty} W(\Pi_N^{in}, \rho^{in}) = 0$

then there exist a unique solution  $\rho^t$  to

$$\partial_t \rho^t(x, v) + v \cdot \nabla_x \rho^t(x, v) + \nabla_v \cdot \left( \rho^t(x, v) \int_{\mathbb{R}^{2d}} \psi(x - y)(v - w) \rho^t(y, w) dy dw \right) = 0$$

this solution belongs to  $L^\infty([0, \infty); \mathcal{P}(\mathbb{R}^{\infty d}))$

and

$$\overline{\lim}_{N \rightarrow \infty} \sup_{t \in [0, \infty)} W(\Pi_N^t, \rho^t) = 0$$

Seung-Yeal Ha, Jeongho Kim, Xiongtao Zhang, Kinetic & Related Models (2018)



# A different approach: Mean field limit by marginals

**Idea:** considering the movement of a generic particle solution to the Liouville equation associated to an Hamiltonian system

Consider the pushforward by the flow  $\Phi^t$  of a compactly supported (symmetric by permutations of the variables N-particles) probability density  $\rho_N^{in}$  on the phase space

$$\Phi^t \# \rho_N^{in} := \rho_N^t$$

which is the solution to the Liouville's equations associated to the system

$$\partial_t \rho_N^t + V \cdot \nabla_X \rho_N^t + \sum_{i=1}^N \nabla_{v_i} \cdot (G_i \rho_N^t) = 0, \quad \rho_N^{t=0} = \rho_N^{in}$$

$$\text{with} \quad G_i = \frac{1}{N} \sum_{j=1}^N \psi(x_i - x_j)(v_j - v_i)$$



# Mean field limit by marginals

To describe the movement of a “generic” particle in the limit of diverging number of particles, we want to perform an average on the  $N$  particles but one. Then, we take the first marginal to the solution to the Liouville equation

$$\rho_{N;1}^t(x, \xi) := \int_{\mathbb{R}^{2(d-1)N}} \rho_N^t(x, \xi, x_2, \xi_2, \dots, x_N, \xi_N) dx_2 d\xi_2 \dots dx_N d\xi_N$$

The marginal approaches the solution to the Vlasov eq.

$$\rho_{N;1}^t(x, \xi) \approx \rho^t$$



# A mean field limit with estimate

## Theorem 1. R.N. - T. Paul, DCDS-B (2022)

Let  $\Phi^t$  be the flow generated by the system (2),  $\psi$  bounded positive nonincreasing Lipschitz continuous, and let  $\rho^t$  be the solution to the Vlasov equation (3) with an initial condition  $\rho^{in} \in L^1(\mathbb{R}^{2d})$  compactly supported. Let moreover  $\rho_{N;1}^t$  be the first marginal of  $\rho_N^t := \Phi^t \# (\rho^{in})^{\otimes N}$ .

Then, for all  $N > 1$ ,  $t \geq 0$ ,

$$W_2(\rho_{N;1}^t, \rho^t) \leq 4\|\psi\|_\infty^2 (2|\bar{v}| + |\text{supp}[\rho^{in}]|) \left( \frac{e^{Lt} - 1}{L} \right)^{\frac{1}{2}} N^{-\frac{1}{2}}$$

with

$$L := 2(1 + 8\|\psi\|_\infty^2 \|v\|_{L^\infty(\text{supp}[\rho^{in}])}^2) \text{ and } \bar{v} = \int v \rho^{in} dx dv$$

where  $\|v\|_{L^\infty(\text{supp}[\rho^{in}])} := \sup_{(x,v) \in \text{supp}[\rho^{in}]} |v|$ .



# Comparison between microscopic and Vlasov

Flocking case

(Simulation by Marta Menci)

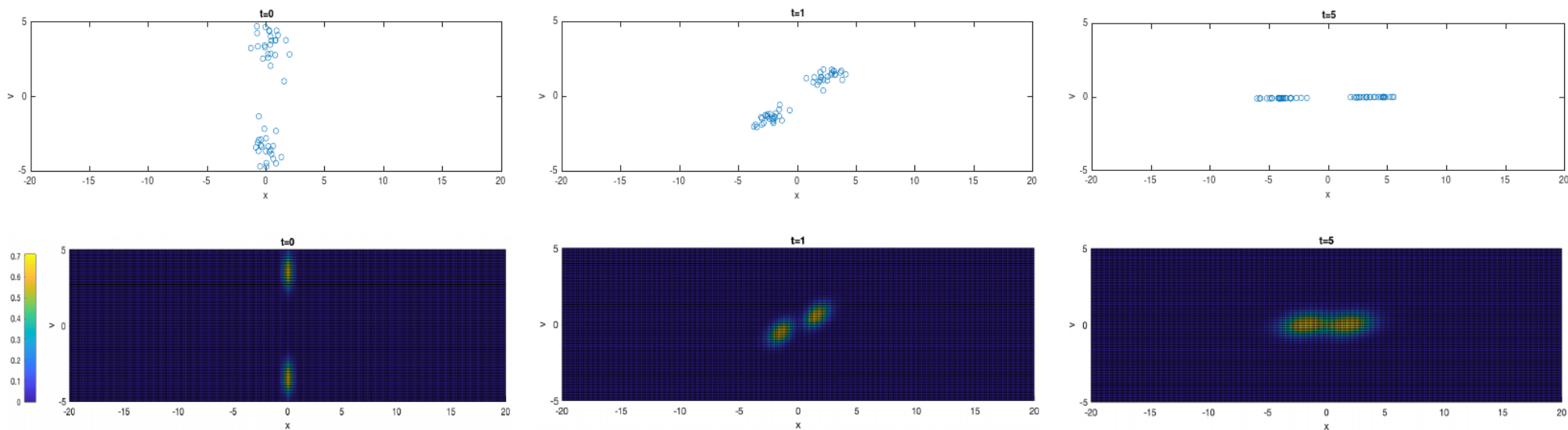


FIGURE 1. Test1: Numerical simulation of Cucker-Smale model with  $\beta = 0.05$ , at particle level (first line) and kinetic (second line) level.



# Comparison between microscopic and Vlasov

Non flocking case

(Simulation by Marta Menci)

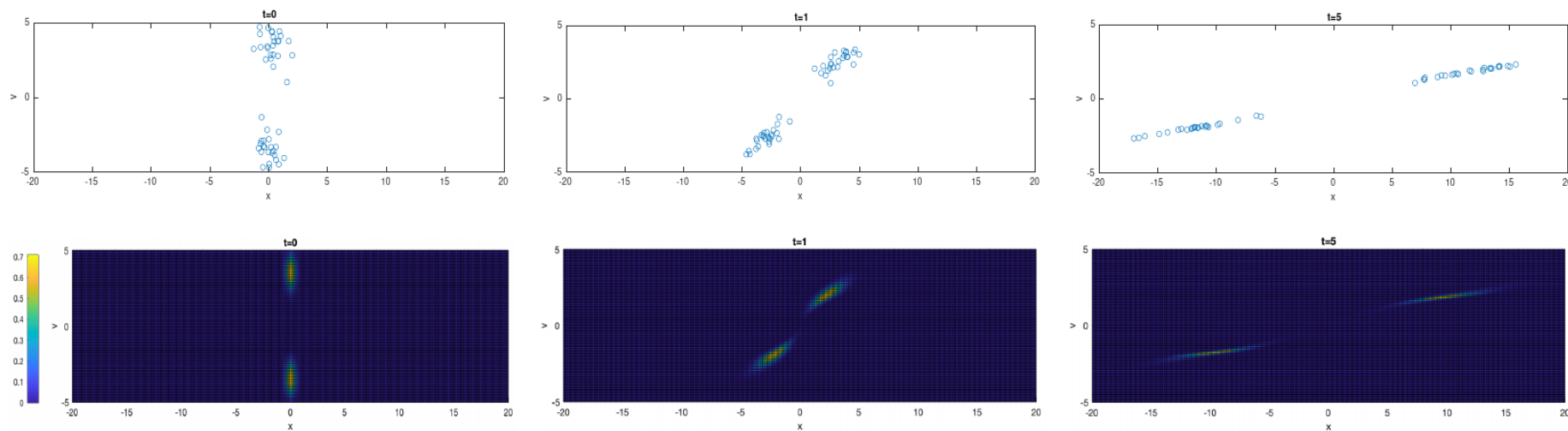


FIGURE 2. Test2: Numerical simulation of Cucker-Smale model with  $\beta = 0.95$ , at particle level (first line) and kinetic (second line) level.





# Come back to chemotaxis

$$(1) \begin{cases} \dot{x}_i = v_i, \\ \dot{v}_i = \frac{1}{N} \sum_{j=1}^N \gamma(v_i - v_j, x_i - x_j) + \eta \nabla_x \varphi^t(x_i) \\ \partial_t \varphi = D \Delta \varphi - \kappa \varphi + f(x, X(t)) \end{cases}$$

- Non local space-time interaction in the Force field
- The associated solution is no more a flow!
- $\rho_N^t = \Phi_N^t \# \rho_N^{in}$  does not satisfy a closed equation (pseudo-Liouville eq.)



# The nonlinear nonlocal Vlasov equation

$$(V) \quad \left\{ \begin{array}{l} \partial_t \rho^t + v \cdot \nabla_x \rho^t = \nabla_v (\nu(t, x, v) \rho^t), \quad \rho^0 = \rho^{in} \in \mathcal{P}(\mathbf{R}^{2d}) \\ \nu(t, x, v) = \gamma * \rho^t(x, v) + \eta \nabla_x \psi^t(x) + F_{ext}(x), \\ \partial_s \psi^s(x) = D \Delta_x \psi - \kappa \psi + g(x, \rho^s), \quad \psi^0 = \varphi^{in}. \\ g(x, \rho^s) = \chi * \rho^s(x). \end{array} \right.$$



# The main convergence theorem

Natalini, Roberto; Paul, Thierry **The mean-field limit for hybrid models of collective motions with chemotaxis.**  
SIAM J. Math. Anal. 55, No. 2, 900-928 (2023)

**Theorem 2.1.** *Let  $\rho^{in}$  be a compactly supported probability on  $\mathbf{R}^{2dN}$ , let  $\Phi_N^t$  be the mapping generated by the particles system (3, 4, 5, 6) as defined by (7), and let  $\tau_{\rho^{in}}$  be the function defined in formula (41) below.*

*Then, for any  $t \geq 0$ ,*

$$W_2 \left( (\Phi_N^t \# (\rho^{in})^{\otimes N})_{N;1}, \rho^t \right)^2 \leq \tau_{\rho^{in}}(t) \begin{cases} N^{-\frac{1}{2}} & d = 1 \\ N^{-\frac{1}{2}} \log N & d = 2 \\ N^{-\frac{1}{d}} & d > 2 \end{cases}$$

*Moreover, let us denote by  $\varphi_{Z^{in}}^t$  the chemical density solution of (3, 4, 5, 6) with initial data  $(Z^{in}, \varphi^{in})$  and by  $\psi_{\rho^{in}}^t$  the one solution of (14, 15, 16, 17) with initial data  $(\rho^{in}, \varphi^{in})$ .*

*Then*

$$\int_{\mathbf{R}^{2dN}} \|\nabla \varphi_{Z^{in}}^t - \nabla \psi_{\rho^{in}}^t\|_{\infty}^2 (\rho^{in})^{\otimes N}(dZ^{in}) \leq \tau_c(t) \begin{cases} N^{-\frac{1}{2}} & d = 1 \\ N^{-\frac{1}{2}} \log N & d = 2 \\ N^{-\frac{1}{d}} & d > 2 \end{cases}$$



# Comparison between microscopic and Vlasov with chemotaxis

Non flocking case

(Simulation by Marta Menci)

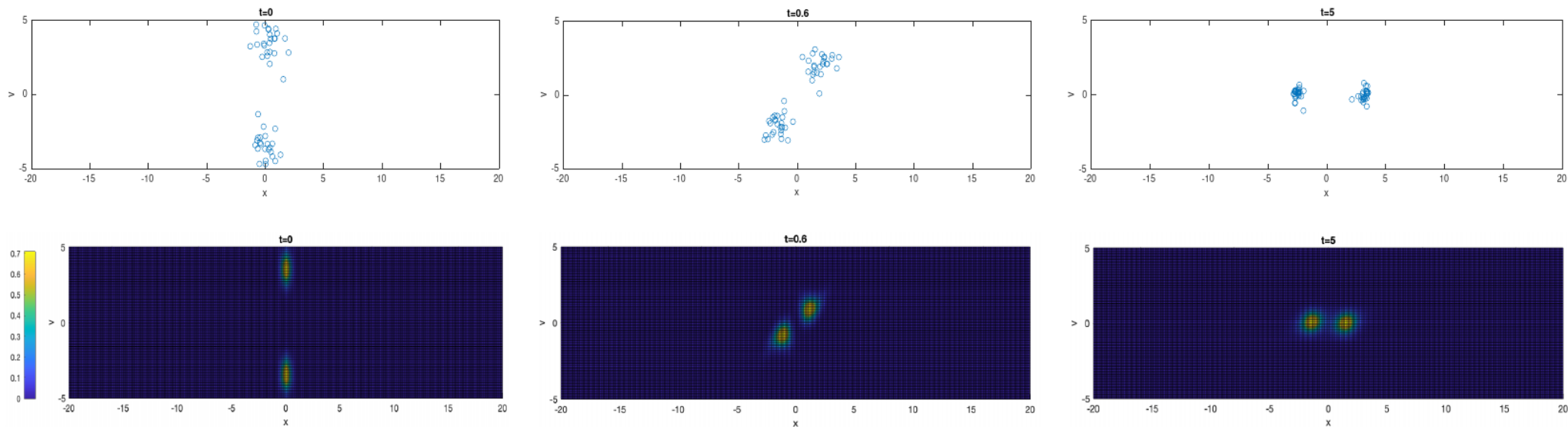


FIGURE 3. Test3: Numerical simulation of Cucker-Smale model with chemotaxis at particle level (first line) and kinetic (second line) level, with  $\beta = 0.95$  and  $\eta = 1.4$ .



# The monokinetic situation

Assume now the initial density is monokinetic  $\rho^{in}(x, v) = \mu^{in}(x)\delta(v - u^{in}(x))$

**Theorem 6.1.** *Let  $\mu^t, u^t, \psi^t$  be a solution to the following system*

$$\begin{cases} \partial_t \mu^t + \nabla(u^t \mu^t) = 0 \\ \partial_t(\mu^t u^t) + \nabla(\mu^t (u^t)^{\otimes 2}) = \mu^t \int \gamma(\cdot - y, u^t(\cdot) - u^t(y)) \mu^t(y) dy + \eta \mu^t \nabla \psi^t + \mu^t F \\ \partial_s \psi^s = D \Delta \psi - \kappa \psi + \chi * \mu^s, \quad s \in [0, t], \\ (\mu^0, u^0, \psi^0) = (\mu^{in}, u^{in}, \psi^{in}) \in H^s, \quad s > \frac{d}{2} + 1. \end{cases}$$

where  $\mu^t, u^t \in C([0, t]; H^s) \cap C^1([0, T]; H^{s-1})$ ,  $\psi^t \in C([0, t]; H^s) \cap C^1([0, T]; H^{s-2}) \cap L^2(0, T; H^{s+1})$  <sup>3</sup>.

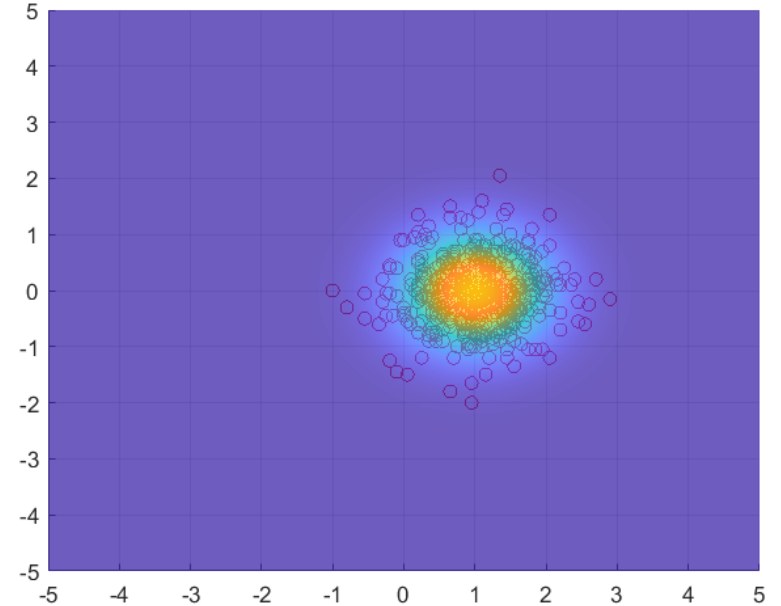
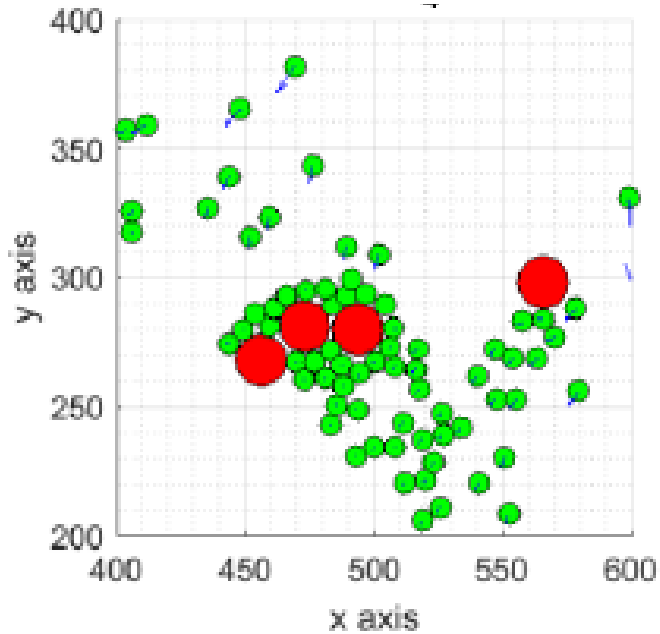
Then  $\rho^t(x, v) := \mu^t(x)\delta(v - u^t(x))$  solves the following system

$$\begin{cases} \partial_t \rho^t + v \cdot \nabla_x \rho^t = \nabla_v(\nu(t, x, v) \rho^t), \\ \nu(t, x, v) = \gamma(x, v) * \rho^t + \eta \nabla_x \psi^t(x) + F_{ext}(x), \\ \partial_s \psi^s(z) = D \Delta_z \psi - \kappa \psi + g(z, \rho^s), \quad \psi^0 = \psi^{in}, \\ \rho^0(x, v) = \mu^{in}(x)\delta(v - u^{in}(x)). \end{cases}$$



# Looking for a good macroscopic model

Marta Menci, Roberto Natalini, Thierry Paul, MICROSCOPIC, KINETIC AND HYDRODYNAMIC  
HYBRID MODELS OF COLLECTIVE MOTIONS WITH CHEMOTAXIS: A NUMERICAL STUDY, preprint 2023



# Comparison between Vlasov and the Hydrodynamic model

Nonlocal Vlasov equation:

$$\left\{ \begin{array}{l} \partial_t \rho^t + v \partial_x \rho^t = \partial_v (\nu(t, x, v) \rho^t), \\ \nu(t, x, v) = \int_{\mathbb{R}} \frac{v - w}{(1 + |x - y|^2)^\beta} \rho^t(y, w) dy dw + \eta \partial_x \psi^t(x) - \alpha v, \\ \partial_s \psi^s(x) = D \partial_x^2 \psi - \kappa \psi + \int_{\mathbb{R}} \int_{x-R}^{x+R} \rho^s(y) dy d\xi, \end{array} \right.$$

Our nonlocal hydrodynamic equation:

$$\left\{ \begin{array}{l} \partial_t \mu^t + \partial_x (u^t \mu^t) = 0 \\ \partial_t (\mu^t u^t) + \partial_x (\mu^t (u^t)^2) = \mu^t \int \gamma(\cdot - y, u^t(\cdot) - u^t(y)) \mu^t(y) dy + \eta \mu^t \partial_x \psi^t - \alpha \mu^t u^t \\ \partial_s \psi^s = D \partial_x^2 \psi - \kappa \psi + \int_{x-R}^{x+R} \mu^s(y) dy, \quad s \in [0, t]. \end{array} \right.$$

Compare the momenta to the hydrodynamic quantities

$$\nu_0^t(x) = \int \rho^t(x, \xi) d\xi \approx \mu^t(x)$$

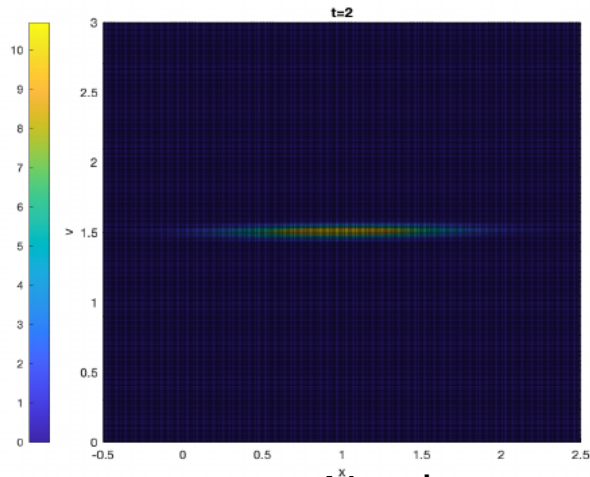
$$\nu_1^t(x) = \int \xi \rho^t(x, \xi) d\xi \approx \mu^t(x) u^t(x)$$



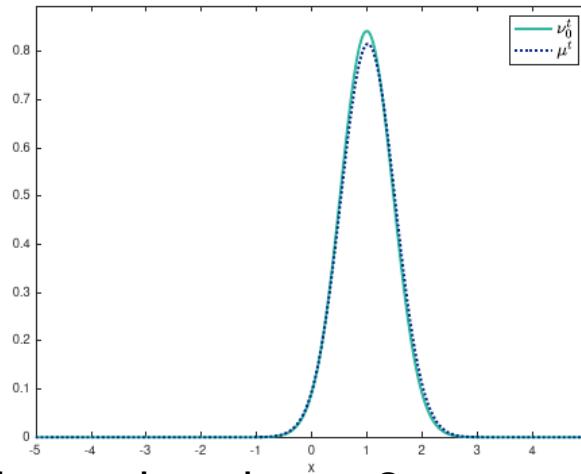
# Comparison between Vlasov and the Hydrodynamic model

The monokinetic case with initial data: 
$$\rho^0(x, v) = \frac{1}{2\pi\sigma_x\sigma_v} e^{-\frac{(x-x_0)^2}{2\sigma_x^2} - \frac{(v-v_0)^2}{2\sigma_v^2}}$$

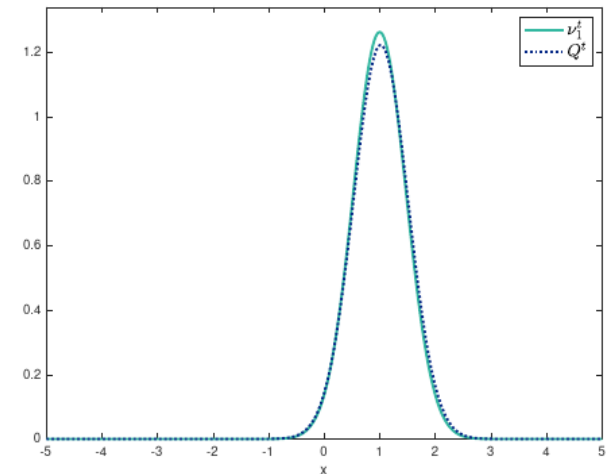
Vlasov phase space



$\nu_0^t$  and  $\mu^t$



$\nu_1^t$  and  $Q^t$



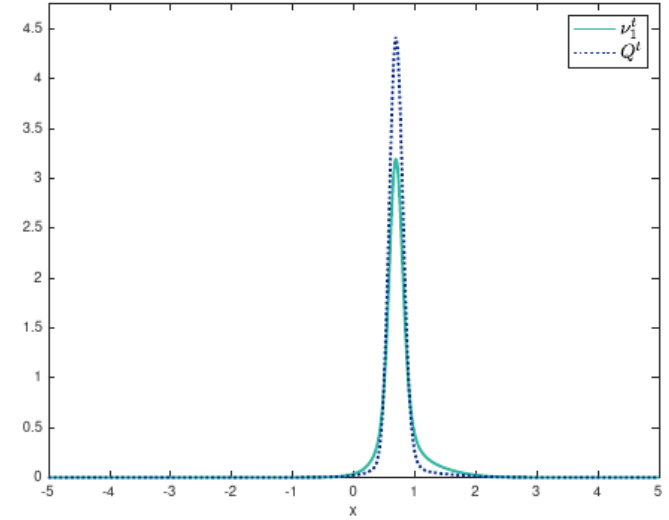
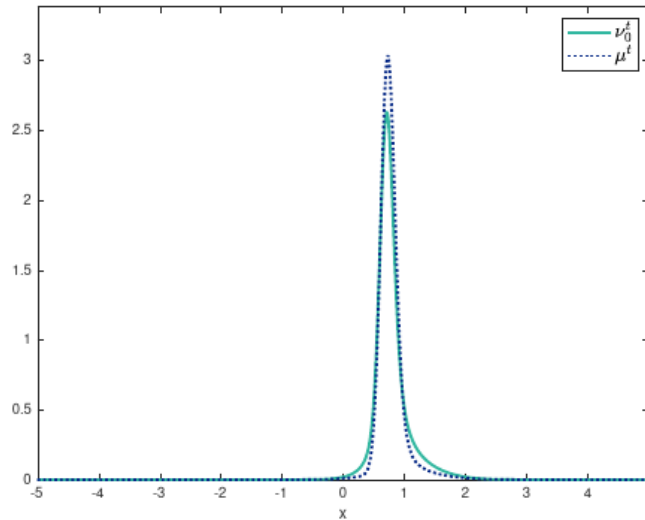
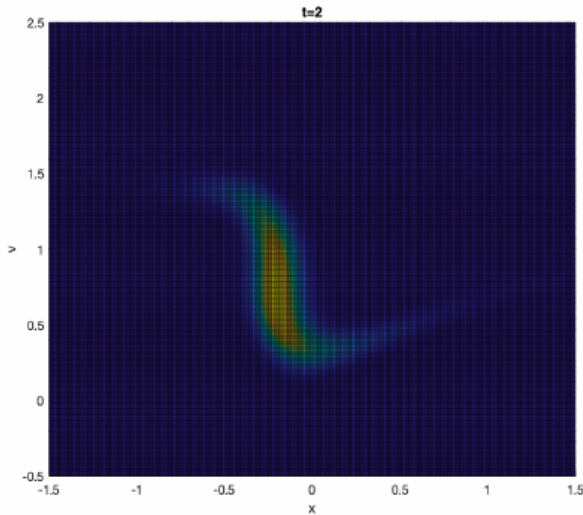
No chemotaxis, no damping, t=2





# Comparison between Vlasov and the Hydrodynamic model

The monokinetic case with initial data: 
$$\rho^0(x, v) = \frac{1}{2\pi\sigma_x\sigma_v} e^{-\frac{(x-x_0)^2}{2\sigma_x^2} - \frac{(v-v_0)^2}{2\sigma_v^2}}$$

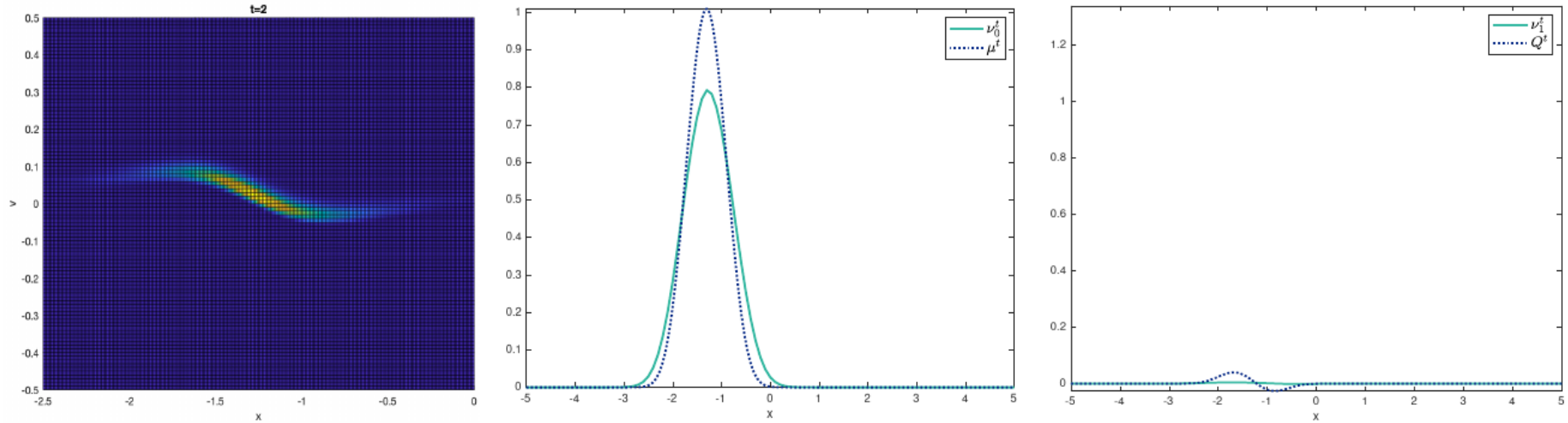


chemotaxis, no damping,  $t=2$ : no longer monokinetic



# Comparison between Vlasov and the Hydrodynamic model

The monokinetic case with initial data: 
$$\rho^0(x, v) = \frac{1}{2\pi\sigma_x\sigma_v} e^{-\frac{(x-x_0)^2}{2\sigma_x^2} - \frac{(v-v_0)^2}{2\sigma_v^2}}$$



chemotaxis, damping,  $t=2$ : dissipation of energy

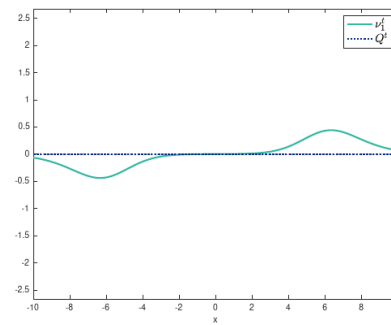
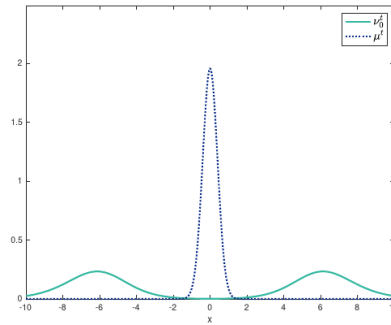


# Comparison between Vlasov and the Hydrodynamic model

The non-monokinetic case with initial data:

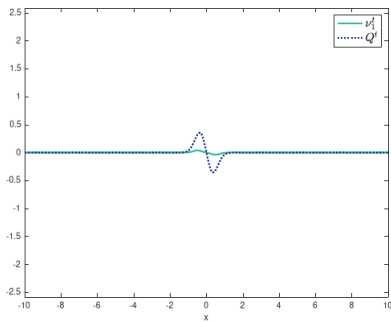
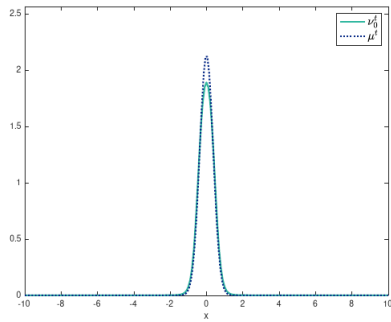
$$\rho^0(x, v) = \frac{1}{2\pi\sigma_x\sigma_v} e^{-\frac{x^2}{2\sigma_x^2}} \left( e^{-\frac{(v+v_0)^2}{2\sigma_v^2}} + e^{-\frac{(v-v_0)^2}{2\sigma_v^2}} \right) \implies u^0(x) = 0$$

No chemotaxis  
No damping  
t=3



No convergence

chemotaxis  
No damping  
t=7



Convergence for  
large times (not  
for all data)



# The Hydrodynamic model with a small pressure term

Our nonlocal hydrodynamic equation with a small pressure (to avoid blow-up)

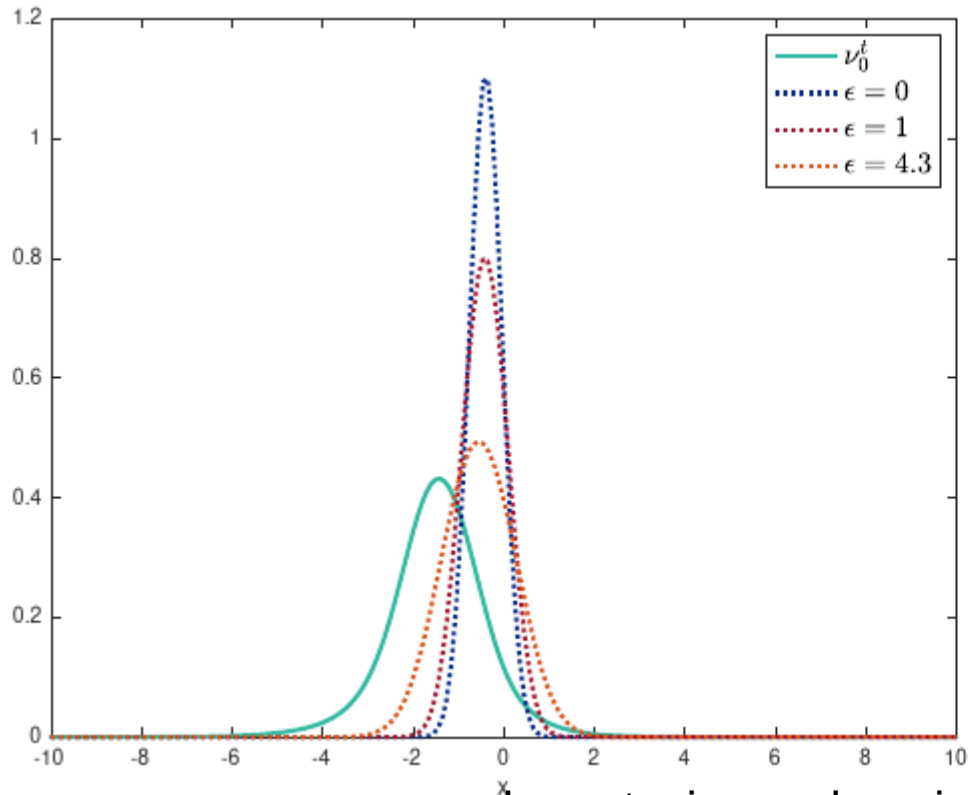
$$\left\{ \begin{array}{l} \partial_t \mu^t + \partial_x (u^t \mu^t) = 0 \\ \partial_t (\mu^t u^t) + \partial_x (\mu^t (u^t)^2 + \varepsilon P(\mu^t)) = \mu^t \int \gamma(\cdot - y, u^t(\cdot) - u^t(y)) \mu^t(y) dy + \eta \mu^t \partial_x \psi^t - \alpha \mu^t u^t \\ \partial_s \psi^s = D \partial_x^2 \psi - \kappa \psi + \int_{x-R}^{x+R} \mu^s(y) dy, \quad s \in [0, t]. \end{array} \right.$$

Compare with the Preziosi-Euler model for chemotaxis in vasculogenesis

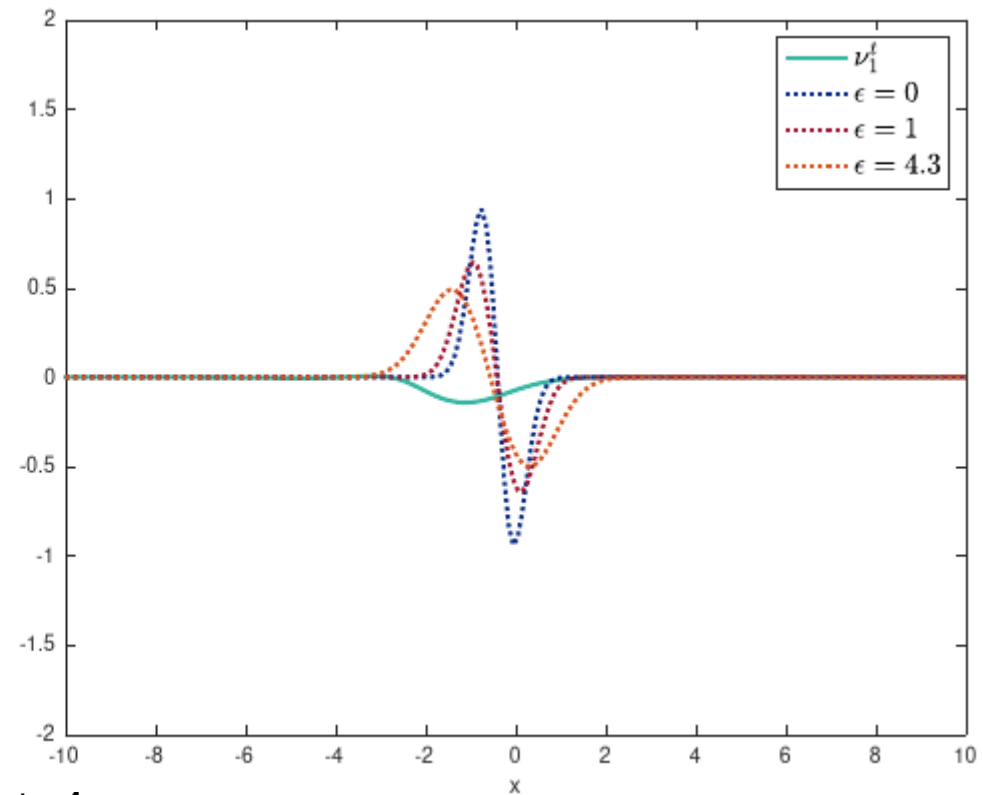
$$\left\{ \begin{array}{l} \partial_t \mu^t + \partial_x (u^t \mu^t) = 0 \\ \partial_t (\mu^t u^t) + \partial_x (\mu^t (u^t)^2 + P(\mu^t)) = +\eta \mu^t \partial_x \psi^t - \alpha \mu^t u^t \\ \partial_s \psi^s = D \partial_x^2 \psi - \kappa \psi + \mu^t. \end{array} \right.$$



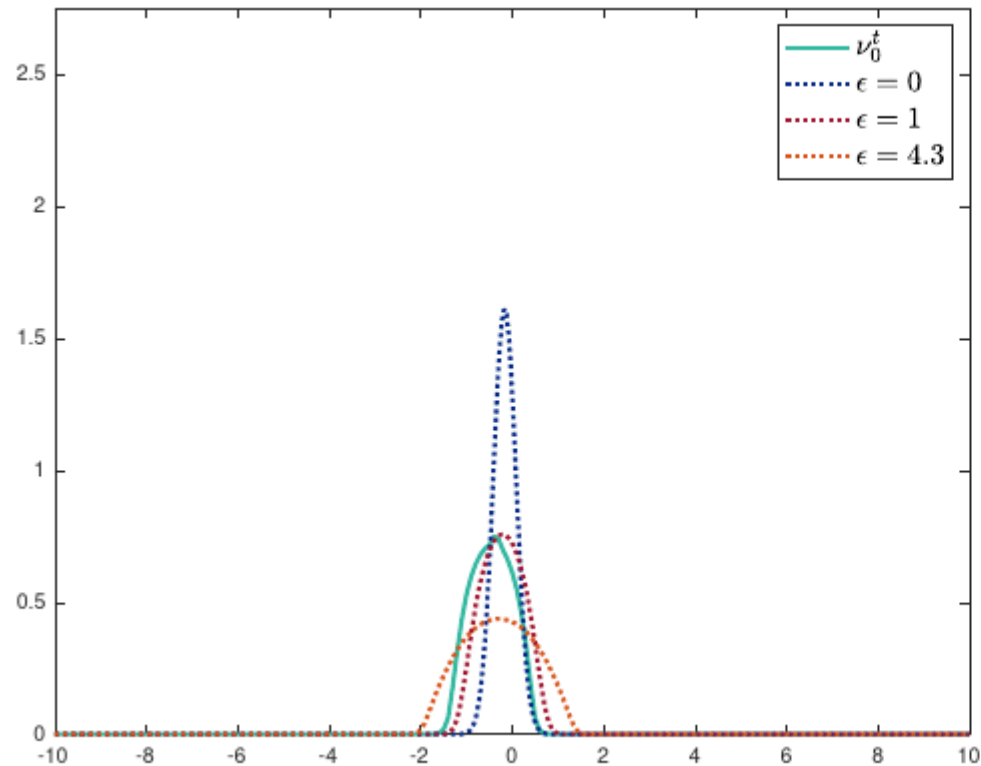
# Comparison between Vlasov and the Hydrodynamic model



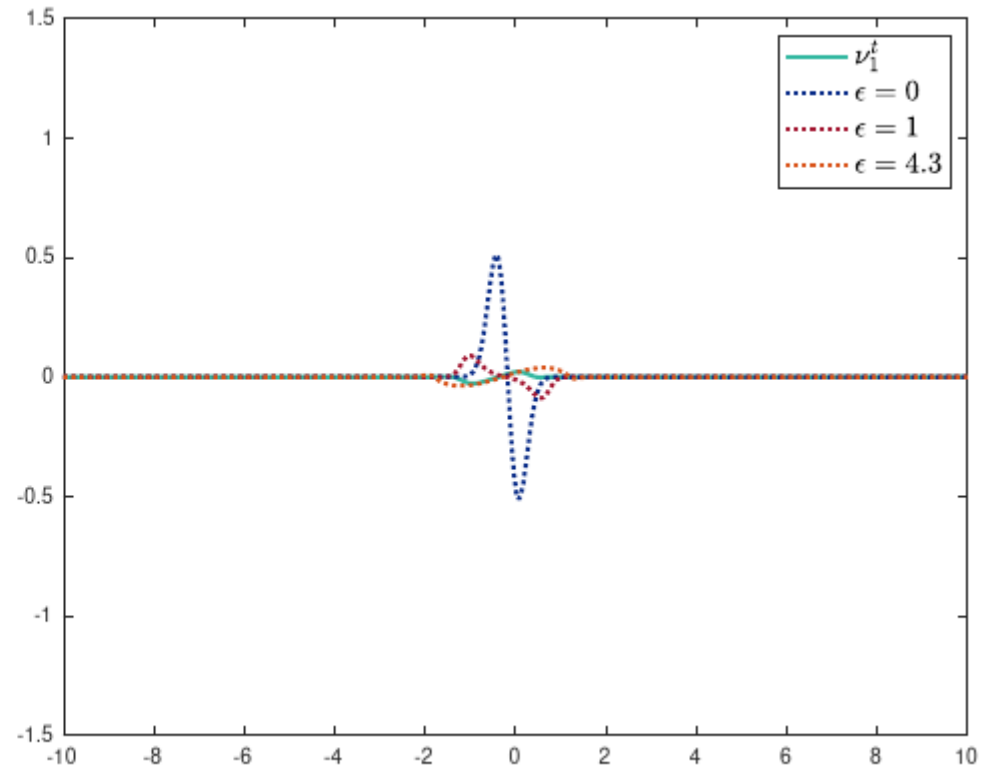
chemotaxis, no damping,  $t=4$



# Comparison between Vlasov and the Hydrodynamic model



chemotaxis, damping,  $t=4$



# Conclusions

- The Vlasov model gives a reliable approximation of the microscopic case
- The Hydrodynamic non local model is a good approximation in the monokinetic case before blow-up (pressureless gas). And in general the Vlasov remains monokinetic only for short times
- Adding a (small) pressure, in the spirit of Preziosi, takes into account for the neglected momenta, but only for certain values of epsilon.
- Damping, which is a natural ingredient in these models even at the microscopic scale, helps a lot in keeping the hydrodynamics near the kinetic.



# Some references

- Di Costanzo E., Natalini R., Preziosi L. A hybrid mathematical model for self-organizing tissue migration in the zebrafish lateral line, *Journal of Mathematical Biology*, 71(1):171–214, 2015
- Braun E.C., Bretti G., Natalini R. Mass-Preserving Approximation of a Chemotaxis Multi-Domain Transmission Model for Microfluidic Chips. *Mathematics*, 9(6)688, 1–34, 2021
- Gabriella Bretti, Adele De Ninno, Roberto Natalini, Daniele Peri and Nicole Roselli, Estimation Algorithm for a Hybrid PDE–ODE Model Inspired by Immunocompetent Cancer-on-Chip Experiment, *Axioms* 2021, 10(4), 243
- Elishan C. Braun, Gabriella Bretti, Roberto Natalini, Parameter estimation techniques for a chemotaxis model inspired by Cancer-on-Chip (COC) experiments, *International Journal of Non-Linear Mechanics*, Volume 140, April 2022, 103895 <https://doi.org/10.1016/j.ijnonlinmec.2021.103895>
- Roberto Natalini, Thierry Paul, On The Mean Field limit for Cucker-Smale models, *Discrete & Continuous Dynamical Systems – B*, 2022, 27(5): 2873-2889. doi: 10.3934/dcdsb.2021164
- Roberto Natalini, Thierry Paul, The Mean-Field limit for hybrid models of collective motions with chemotaxis, *SIAM J. Math. Anal.* 55, No. 2, 900-928 (2023)
- Marta Menci, Roberto Natalini, Thierry Paul, MICROSCOPIC, KINETIC AND HYDRODYNAMIC
- HYBRID MODELS OF COLLECTIVE MOTIONS WITH CHEMOTAXIS: A NUMERICAL STUDY, preprint 2023





Ciao Maurizio!



**NONLINEAR PARTIAL DIFFERENTIAL EQUATIONS**  
A conference in memory of Maurizio Falcone